

X-ray transitions in highly charged neonlike ions

P. Beiersdorfer, S. von Goeler, M. Bitter, E. Hinnov, R. Bell, S. Bernabei, J. Felt, K. W. Hill, R. Hulse, J. Stevens, S. Suckewer, J. Timberlake, and A. Wouters

Plasma Physics Laboratory, Princeton University, Princeton, New Jersey 08544

M. H. Chen, J. H. Scofield, D. D. Dietrich, M. Gerassimenko, E. Silver, and R. S. Walling

Lawrence Livermore National Laboratory, University of California, Livermore, California 94550

P. L. Hagelstein

Electronics Laboratory, Massachusetts Institute of Technology, Cambridge, Massachusetts 02139

(Received 20 October 1987)

Wavelength measurements of $n=3$ to $n=2$ transitions in neonlike Xe^{44+} , La^{47+} , Nd^{50+} , and Eu^{53+} have been made using a high-resolution Bragg-crystal spectrometer on the Princeton Large Torus tokamak. The measurements cover the wavelength regions 2.00–3.00 Å and include the electric dipole and the electric and magnetic quadrupole transitions. The measured wavelengths are compared to energy levels obtained from a multiconfigurational Dirac-Fock calculation. Systematic differences between the experimental and theoretical values are found, which vary smoothly with atomic number. The magnitude of the differences depends on the particular type of transition and ranges from -2.8 eV to $+2.2$ eV. Inclusion of electron correlation corrections due to ground-state correlations and (super-) Coster-Kronig-type fluctuations in the theoretical energies is shown to reduce the differences for some but not all types of transitions.

I. INTRODUCTION

The spectra of very highly charged ions can provide detailed information on the structure of multielectron systems in a strong Coulomb field. Therefore, high-resolution wavelength measurements of spectral lines emitted from few-electron, high- Z systems can be used to check the accuracy of multiconfigurational relativistic atomic structure calculations.

Systematic comparisons between experimental and theoretical transition energies have been made recently by Seely *et al.* for $4p \rightarrow 4s$ transitions in copperlike ions and for $3d \rightarrow 3p$ transitions in cobaltlike ions for elements up to uranium.¹ In the case of the cobaltlike transitions the comparison between experimental observations and theoretical values from Dirac-Fock calculations showed a discrepancy of about 3 eV. This discrepancy has since been removed by including electron correlation corrections to the theoretical transition energies.²

High-resolution data on $\Delta n = 1$ x-ray transitions in multielectron systems such as the $3 \rightarrow 2$ x-ray transitions in neonlike systems have been obtained only recently, and the existing data show some disagreement with theoretical wavelengths. A high-resolution measurement of the $3 \rightarrow 2$ transitions in neonlike silver has been made on the Princeton Large Torus (PLT).³ The measurements showed systematic discrepancies between observed and calculated wavelengths which depended on the type of transition. It was found that the experimental wavelengths of the $3p, 3s \rightarrow 2p$ transitions were shorter than the values predicted by a relativistic atomic structure calculation.³ The experimental wavelengths of the $3d \rightarrow 2p$ transitions were determined to be slightly longer, and

those of the $3p \rightarrow 2s$ transitions considerably longer than the predicted values.³ Similar discrepancies between experimental and theoretical wavelengths of the $3p \rightarrow 2s$ transitions were inferred from observations of the x-ray transitions in neonlike bismuth in beam-foil experiments.⁴ The authors speculated that this discrepancy may be due to inadequacies in the calculation of quantum-electrodynamical corrections, in particular, of the self-energy. However, the experimental uncertainties of about 6 eV were too large to obtain a definite result. The small amount of high-resolution data obtained to date has so far been insufficient to perform a detailed comparison of theory and experiment as a function of atomic number Z .

In this paper we extend the high-resolution measurements of the $3 \rightarrow 2$ transitions in neonlike silver ($Z = 47$) made previously³ to the rare-earth elements. In particular, we report on measurements of the $\Delta n = 1$ electric dipole, electric quadrupole, and magnetic quadrupole transitions of neonlike xenon ($Z = 54$), lanthanum ($Z = 57$), neodymium ($Z = 60$), and europium ($Z = 63$), which fall into the x-ray region between 2.00–2.19 and 2.29–3.00 Å. The spectra were observed on PLT from discharges with high electron temperatures of up to 6.5 keV and were made using the high-resolution Bragg-crystal spectrometer. The uncertainty in the wavelength measurements is ± 0.1 mÅ for most transitions and corresponds to a relative error of $\Delta\lambda/\lambda \approx 1/20000$.

The data presented in this paper have allowed us to make detailed comparisons between the experimental results and theoretical values which have been obtained from a multiconfigurational Dirac-Fock (MCDF) code developed by Grant and co-workers,^{5,6} and which include QED corrections. Although the agreement is generally

excellent, small yet significant differences have been found, which, as in the case of silver,³ depend on the type of transition. The magnitude of the differences ranges from about +2.2 eV for transitions of the type $3p, 3s \rightarrow 2p$ to as much as -2.8 eV for transitions of the type $3d, 3p \rightarrow 2s$. In order to understand these discrepancies we have also made a simple estimate of the residual electron correlation energy arising from electron ground-state correlations and from (super-) Coster-Kronig-type fluctuations. We find that including the estimate for the residual electron correlation energy in the theoretical transition energies reduces the differences between theoretical and experimental wavelengths for many transitions. However, the residual electron correlation energy cannot account for all differences, and considerable discrepancies remain for some types of transitions.

II. EXPERIMENTAL ARRANGEMENT

The $n = 3$ to $n = 2$ transitions in Xe^{44+} , La^{47+} , Nd^{50+} , and Eu^{53+} were measured using the PLT high-resolution Bragg-crystal spectrometer in Johann geometry.⁷ The spectrometer employs a $11 \times 3\frac{3}{4} \times 0.06$ -in³ silicon crystal cut to the (220) plane with a $2d_\infty$ spacing of 3.8400 Å and bent to a radius of curvature of 365 cm. Most measurements were performed with the illuminated length of the crystal varying between 2.5 and 10 cm. In the region below 2.19 Å an illuminated length of about 18 cm was used, in order to maintain an adequate count rate during the measurements of europium. The detector is oriented perpendicular to the line connecting the crystal and the center of the detector, and not tangent to the Rowland circle, as described in Refs. 3 and 7. As a result, the best focus is achieved in the center of the detector, and the resolution decreases toward the edges. In the wavelength range of interest, 2.00–3.00 Å, the resolution of the central part of the spectrum varied from $\lambda/\Delta\lambda \approx 1200$ to $\lambda/\Delta\lambda \approx 8000$. For comparison, the Doppler-broadened linewidth of xenon corresponded to $\lambda/\Delta\lambda \approx 5000$ at ion temperatures of 1 keV, which were typical for the plasma conditions. Six settings were necessary to span the wavelength regions 2.00–2.19 and 2.29–3.00 Å. No measurements were taken in the region between 2.19 and 2.29 Å due to insufficient machine time.

The minimum central electron temperature necessary to observe $3 \rightarrow 2$ transitions of a given neonlike ion with our instrument on PLT is shown in Fig. 1. The maximum central electron temperature achieved in PLT was approximately 6.5 keV as determined by Thomson scattering. This temperature enabled us to observe the transitions between the $(2p_{3/2}^5 3s_{1/2})_{J=1,2}$ upper states and the ground state in Eu^{53+} , although the signal was faint. The line-averaged electron density in these discharges was 1.0×10^{13} cm³. The high electron temperatures were obtained with a modest amount of lower-hybrid, radio-frequency heating power, $P_{\text{LH}} \approx 650$ kW, using a side-launching, 16-grill waveguide.^{8,9}

At each electron temperature shown in Fig. 1 a certain fractional abundance of the corresponding neonlike ions is reached in the center of the plasma. For instance, according to coronal equilibrium values of Breton *et al.*,¹⁰

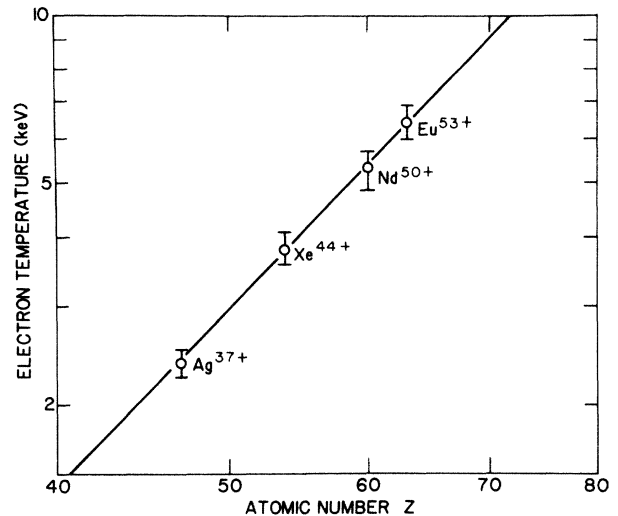


FIG. 1. Minimum central electron temperature necessary to observe x-ray transitions in neonlike ions of atomic number Z with the PLT high-resolution Bragg-crystal spectrometer. The line-averaged electron density in each case was 1×10^{13} cm⁻³. The solid line is drawn as a visual aid only.

the electron temperature of 3.8 keV corresponds to a fractional abundance of about 8% of xenon in the neonlike state, Xe^{44+} . Similar neonlike ion fractions are predicted by coronal equilibrium calculations for silver, neodymium, and europium. Coronal equilibrium calculations, however, overestimate the actual abundance in a tokamak plasma. A more realistic equilibrium calculation which includes plasma transport and charge-exchange recombination with neutral hydrogen predicts lower fractions of neonlike ions in PLT plasmas.¹¹

Lanthanum, neodymium, and europium were injected into PLT plasmas via laser blowoff.¹² Xenon was puffed into the plasma using a fast gas valve. Concurrently with xenon, argon and scandium have been introduced into the plasma in order to use the hydrogenlike resonance lines as wavelength references. Furthermore, titanium, chromium, manganese, and a small amount of vanadium were indigenous to the plasma, and the hydrogenlike and heliumlike spectra of these elements have also been recorded.

III. EXPERIMENTAL RESULTS

An overview of the spectral range investigated is given in Fig. 2, which shows the location of the main $\Delta n = 1$ neonlike lines as well as the location of the various hydrogenlike and heliumlike spectra which were observed. We have normalized our measurements to the theoretical values for the hydrogenic transitions given in Refs. 13–15 since these wavelengths can be calculated with the highest accuracy.^{13–16}

The experimental values of the wavelengths of the $3s, 3p, 3d \rightarrow 2p$ and $3d, 3p \rightarrow 2s$ transitions are listed in Table I. They have been determined with respect to the theoretical wavelength values of the hydrogenic lines given in Table II. The procedures used to identify the

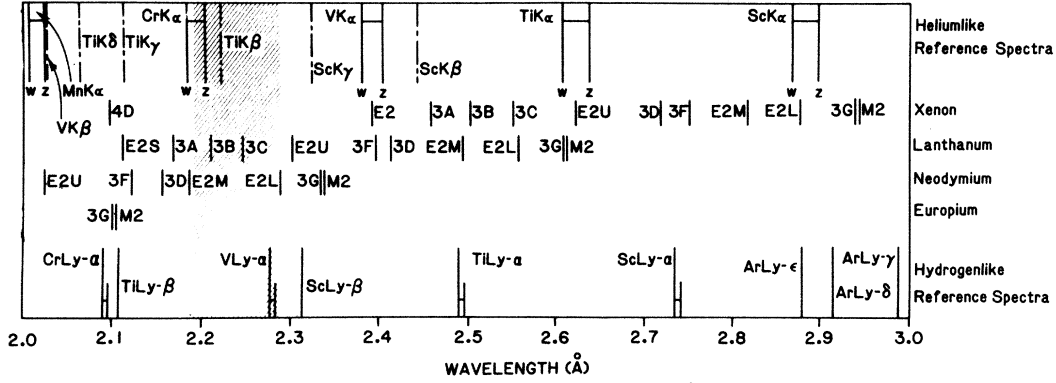


FIG. 2. Overview of the spectra observed in the wavelength range 2.00–3.00 Å showing the location of the x-ray transitions in neonlike xenon, lanthanum, neodymium, and europium with respect to the location of various hydrogenlike and heliumlike reference lines. The notation used to label the neonlike transitions is that of Table I. No measurements were made in the interval 2.19–2.29 Å (shaded region).

neonlike transitions and to determine their respective wavelengths are similar to those described in Ref. 3 for the measurement of Ag^{37+} . The errors in the wavelengths of the strong neonlike lines ($\pm 0.1 \text{ m}\text{\AA}$) are due to uncertainties in the dispersion, which is determined by the geometry of a given spectrometer setting, while the

error of weak lines is predominantly given by the statistical errors at low count rates. The dispersion was checked by measuring the wavelength of several hydrogenic lines relative to other hydrogenic lines as a reference. For example, the scandium line $\text{Ly-}\beta_1$ was measured relative to the titanium line $\text{Ly-}\alpha_1$ as a reference, and its measured

TABLE I. Experimental wavelengths of the x-ray transitions observed in Xe^{44+} , La^{47+} , Nd^{50+} , and Eu^{53+} . Each wavelength is determined with respect to the wavelength of the hydrogenic reference line listed in the last column. The experimental uncertainties are indicated in parentheses, e.g., 2.4601(1) means 2.4601 ± 0.0001 .

Element	Upper level	Key	$\lambda_{\text{expt}}^{\text{a}}$ (Å)	λ_{expt} (Å)	Reference line
Xenon	$(2p_{3/2}^5 3s_{1/2})_{J=2}$	M2	2.9449(1)		Ar Ly- δ
	$(2p_{3/2}^5 3s_{1/2})_{J=1}$	3G	2.9411(1)	2.938 ^b	Ar Ly- δ
	$(2p_{3/2}^5 3p_{1/2})_{J=2}$	E2L	2.8799(1)		Ar Ly- ϵ
	$(2p_{3/2}^5 3p_{3/2})_{J=2}$	E2M	2.8186(1)		Ar Ly- ϵ
	$(2p_{1/2}^5 3s_{1/2})_{J=1}$	3F	2.7288(1)	2.726 ^b	Sc Ly- α_1
	$(2p_{3/2}^5 3d_{5/2})_{J=1}$	3D	2.7203(1)	2.717 ^b	Sc Ly- α_1
	$(2p_{1/2}^5 3p_{3/2})_{J=2}$	E2U	2.6221(2.5)		Ti Ly- α_1
	$(2p_{1/2}^5 3d_{3/2})_{J=1}$	3C	2.5525(1)	2.551 ^b	Ti Ly- α_1
	$(2s_{1/2} 3p_{1/2})_{J=1}$	3B	2.5052(1.5)		Ti Ly- α_1
	$(2s_{1/2} 3p_{3/2})_{J=1}$	3A	2.4601(1)		Ti Ly- α_1
Lanthanum	$(2s_{1/2} 3d_{5/2})_{J=2}$	E2S	2.3941(1)		Sc Ly- β_1
	$(2p_{3/2}^5 4d_{5/2})_{J=1}$	4D	2.0957(1)		Cr Ly- α_1
	$(2p_{3/2}^5 3s_{1/2})_{J=2}$	M2	2.6133(1)		Ti Ly- α_1
	$(2p_{3/2}^5 3s_{1/2})_{J=1}$	3G	2.6100(2)	2.6142 ^c	Ti Ly- α_1
	$(2p_{3/2}^5 3p_{1/2})_{J=2}$	E2L	2.5580(1)		Ti Ly- α_1
	$(2p_{3/2}^5 3d_{5/2})_{J=1}$	3D	2.4139(1)	2.4149 ^c	Sc Ly- β_1
	$(2p_{1/2}^5 3s_{1/2})_{J=1}$	3F	2.3965(1)		Sc Ly- β_1
	$(2p_{1/2}^5 3p_{3/2})_{J=2}$	E2U	2.3019(2)		Sc Ly- β_1
Neodymium	$(2s_{1/2} 3p_{3/2})_{J=1}$	3A	2.1671(1.5)	2.1687 ^c	Cr Ly- α_1
	$(2s_{1/2} 3d_{5/2})_{J=2}$	E2S	2.1108(1.5)		Cr Ly- α_1
	$(2p_{3/2}^5 3s_{1/2})_{J=2}$	M2	2.3359(1)		Sc Ly- β_1
	$(2p_{3/2}^5 3s_{1/2})_{J=1}$	3G	2.3331(1)		Sc Ly- β_1
Europium	$(2p_{3/2}^5 3d_{5/2})_{J=1}$	3D	2.1543(1.5)	2.1573 ^c	Cr Ly- α_1
	$(2p_{1/2}^5 3s_{1/2})_{J=1}$	3F	2.1206(1.5)		Cr Ly- α_1
	$(2p_{3/2}^5 3s_{1/2})_{J=2}$	M2	2.1015(2)		Sc Ly- β_1
	$(2p_{3/2}^5 3s_{1/2})_{J=1}$	3G	2.0990(2)		Cr Ly- α_1

^aPresent measurement.

^bConturie *et al.*, Ref. 21.

^cAglitskii *et al.*, Ref. 22.

TABLE II. Wavelengths of the hydrogenic transitions used as references in the measurement of the neonlike transitions. $\langle \rangle$ denotes average.

Reference line	Transition	λ_{theory} (Å)
Ar Ly- δ	$5P_{3/2} \rightarrow 1S_{1/2}$, $5P_{1/2} \rightarrow 1S_{1/2}$	$\langle 2.917\,56 \rangle^a$
Ar Ly- ϵ	$6P_{3/2} \rightarrow 1S_{1/2}$, $6P_{1/2} \rightarrow 1S_{1/2}$	$\langle 2.880\,95 \rangle^a$
Sc Ly- α_1	$2P_{3/2} \rightarrow 1S_{1/2}$	2.736 02 ^b
Ti Ly- α_1	$2P_{3/2} \rightarrow 1S_{1/2}$	2.491 20 ^b
Sc Ly- β_1	$3P_{3/2} \rightarrow 1S_{1/2}$	2.310 66 ^c
Cr Ly- α_1	$2P_{3/2} \rightarrow 1S_{1/2}$	2.090 14 ^b

^aGarcia and Mack, Ref. 13.

^bJohnson and Soff, Ref. 15.

^cErickson, Ref. 14.

wavelength was found to agree with the theoretical value of Ref. 14 to within 0.02 mÅ. Similarly, the wavelengths of heliumlike lines were measured relative to other heliumlike lines as references. The agreement of the measured and predicted wavelengths of the heliumlike lines was better than 0.1 mÅ. A few neonlike transitions have been observed in different settings of the spectrometer (corresponding to different instrumental dispersion and different hydrogenic reference lines), and the wavelengths were reproducible to within 0.1 mÅ. We note, however, that an upper limit is placed on the experimental certainty with which wavelengths can be determined by the presence of unresolved, high- n dielectronic satellites.¹⁷ High- n satellites tend to shift the wavelength of the apparent resonance line and thus can affect the position of the hydrogenic reference lines as well as the position of the neonlike lines. This process has been studied for hydrogenlike and heliumlike resonance lines^{18,19} and was found to cause shifts which are typically less than about 0.1 mÅ.^{18,19} We have measured the wavelengths of the heliumlike resonance lines $1snp\ ^1P_1 \rightarrow 1s^2\ ^1S_0$ of scandium, titanium, vanadium, and chromium relative to the hydrogenic reference lines, and we have compared the data to theoretical values. For all nine heliumlike resonance lines (cf. Fig. 2) the measured wavelengths are systematically between 0.1 and 0.2 mÅ shorter than the values predicted by Vainshtein and Safronova.²⁰ A similar discrepancy between measured and calculated values for the heliumlike resonance lines had been reported earlier.³ If we assume that the accuracy of the calculations of Vainshtein and Safronova²⁰ is better than 0.1 mÅ, then the discrepancy would indicate a systematic experimental error of 0.1–0.2 mÅ. On the other hand, it is also possible that the theoretical heliumlike wavelengths computed by Vainshtein and Safronova²⁰ are somewhat too long, or, though less likely, that wavelength shifts of the hydrogenlike and heliumlike resonance lines due to contributions from unresolved satellites are (very) different at a given electron temperature.

Typical spectra data are shown in Figs. 3 and 4 for the case of neodymium. The spectrum in Fig. 3 contains transitions of the type $3s_{1/2} \rightarrow 2p_{3/2}$. The neonlike doublet ($2p_{3/2}^5 3s_{1/2}$) $_{J=1,2} \rightarrow 2p^6$, denoted 3G and M2, is readily identifiable. In addition, an array of sodiumlike,

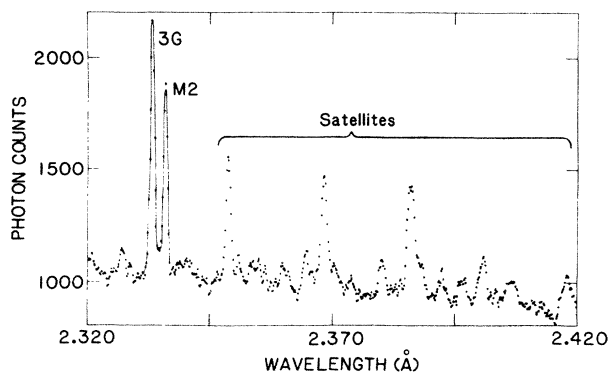


FIG. 3. Spectrum of the $3s_{1/2} \rightarrow 2p_{3/2}$ transitions, labeled 3G and M2, in Nd^{50+} . The spectrum was obtained with the PLT high-resolution spectrometer. Also seen are satellites due to $3s_{1/2} \rightarrow 2p_{5/2}$ transitions in lower charge states of neodymium. The data have been accumulated from 33 PLT discharges. The background is due to the bremsstrahlung and recombination continuum.

magnesiumlike, and possibly aluminumlike satellites can be seen on the long-wavelength side of these lines. The ratio of the satellite line intensity to the intensity of the neonlike lines in this case is considerably larger than the ratio observed previously in the spectrum of silver,³ and may indicate a greater abundance of ions in the lower charge states. The spectrum of the electric dipole transition $3s_{1/2} \rightarrow 2p_{1/2}$, labeled 3F, and of the electric dipole transition $3d_{5/2} \rightarrow 2p_{3/2}$, labeled 3D, is shown in Fig. 4. Again strong satellites due to the corresponding transitions in ions in lower ionization states are seen in the spectrum. Since the detector is not tangent to the Rowland circle, but instead is oriented perpendicular to the line connecting the crystal and the center of the detector, the spectral regions observed with the edges of the detector have lower resolution than those observed with the

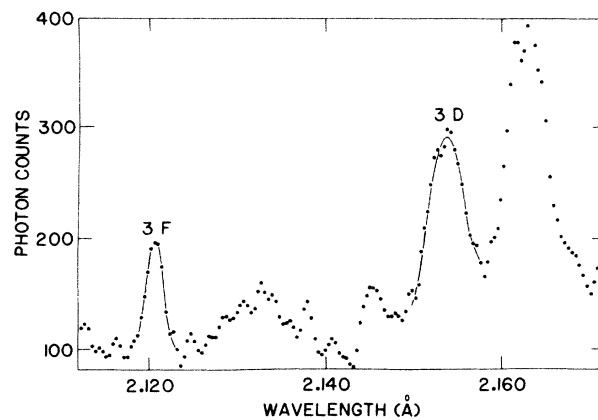


FIG. 4. Spectrum of the transition $3s_{1/2} \rightarrow 2p_{1/2}$, labeled 3F and $3d_{5/2} \rightarrow 2p_{3/2}$, labeled 3D, in Nd^{50+} . The data have been accumulated from 13 PLT discharges. For elements with $Z \geq 55$ the wavelength of line 3F is shorter than the wavelength of line 3D as a result of the relativistic splitting of the $2p_{3/2}^5$ and $2p_{1/2}^5$ core levels. The increased linewidth of line 3D compared to line 3F is due to a diminished resolution of the spectrometer.

central part of the detector. This effect is especially strong in Fig. 4, where the width of line $3D$ is much larger than the width of line $3F$.

Subtraction of background spectra, as described earlier in Ref. 3, was required in only a few cases. The most notable case is due to a coincidence of line $3G$ in lanthanum with the resonance transition $1s2p\ ^1P_1 \rightarrow 1s^2\ ^1S_0$ in Ti^{20+} . As a result, the uncertainty of the measured wavelength of this line is larger than that of most other electric dipole lines.

All but one of the strong electric dipole transitions in neonlike xenon have been measured previously by Conturie *et al.* from laser-irradiated, imploding microballoons,²¹ and several of the strong electric dipole transitions in lanthanum and neodymium have been measured by Aglitskii *et al.* in vacuum spark discharges.²² The results of these measurements are listed in Table I for comparison. In all cases our values disagree with these prior measurements by several milliangstroms. This disagreement is somewhat larger than the errors of 2 mÅ quoted in Ref. 21 and the errors of 0.6–3.0 mÅ quoted in Ref. 22. Part of the disagreement could be due to the fact that these authors used different transitions and correspondingly different theoretical wavelength values for the calibration of their wavelength measurements. The disagreement may also reflect a possible contamination of the neonlike lines by transitions in lower charge states as a result of the high density and transient nature of laser-produced or spark plasmas.

We have observed two electric quadrupole ($E2$) transitions of the type $3d_{5/2} \rightarrow 2s_{1/2}$, labeled $E2S$. Identification of this type of transition has been reported recently by Gauthier *et al.* in laser-produced plasmas for strontium, molybdenum, rhodium, and silver.²³ Further, we have observed $E2$ transitions of the type $3p \rightarrow 2p$. The longest-wavelength $E2$ line, denoted $E2L$ ("lower"), is relatively intense and thus can easily be identified in the spectrum. The shorter-wavelength $E2$ lines, denoted $E2M$ ("middle") and $E2U$ ("upper"), are the weakest features observed in the present spectra. Both have been identified in the case of xenon; only one of the two has been identified in lanthanum. The shortest-wavelength $E2$ line in xenon, line $E2U$, partially blends with a line which may be due to a transition in a lower charge state, such as aluminumlike or siliconlike xenon. Consequently, the value listed for this line in Table I is less certain

than those of the other electric quadrupole lines in xenon. The electric quadrupole lines of neodymium which fall into the wavelength region monitored in the present experiment coincide with transitions in the $K\alpha$ spectra of heliumlike chromium and manganese. The $E2$ transitions in neodymium could not be identified even if background subtraction techniques were used.

Together with the electric dipole transitions of the type $3s \rightarrow 2p$, the electric quadrupole lines can be used to determine the energies of $\Delta n = 0$ transitions within the $n = 3$ shell. These transitions, in particular the transitions $(2p_{1/2}^5 3p_{3/2})_{J=2} \rightarrow (2p_{1/2}^5 3s_{1/2})_{J=1}$ and $(2p_{3/2}^5 3p_{3/2})_{J=2} \rightarrow (2p_{3/2}^5 3s_{1/2})_{J=1}$, are of interest in collisionally pumped soft x-ray laser schemes.^{24–26} Several of the $3 \rightarrow 3$ intrashell transitions are listed in Table III. A direct measurement of the $3 \rightarrow 3$ transitions is very difficult due to the presence of many lines of nearly identical wavelength which have much higher intensity and which result from $\Delta n = 0$ transitions in sodiumlike, magnesiumlike, and aluminumlike charge states. The values in Table III indicate that the lasing wavelength in a collisionally pumped laser could be reduced to about 58.3 Å if gain were achieved in a lanthanum target, compared to approximately 100 Å in silver,³ and 200 Å in selenium.²⁴

In the case of xenon we can compare our $\Delta n = 0$ results to those obtained by Dietrich *et al.* in beam-foil measurements.²⁷ Table III shows that our values agree with those in Ref. 27 for the three transitions of the type $3p \rightarrow 3s$, while our values for the two $\Delta n = 0$ transitions of the type $3d \rightarrow 3p$ differ from those in Ref. 27 by amounts which are larger than the quoted errors. The discrepancies suggest that there may be systematic errors in either measurement which have not been accounted for. Such errors are likely to be different in each case, as the experimental conditions are very different. In the beam-foil experiment the x-ray lines were simultaneously observed in one spectrum and the energies of the $\Delta n = 0$ transitions were determined from a measurement of the wavelength differences of two x-ray lines using the instrumental dispersion.²⁷ The spectrum had been calibrated by several lines: the $K\alpha_1$, $K\alpha_2$, and $K\beta$ lines of neutral scandium, the $K\alpha_1$ and $K\alpha_2$ lines of neutral titanium, and the $L\alpha_1$ line of neutral lanthanum. In the present experiment, the x-ray lines were recorded with different spectrometer settings, and for each setting their wavelengths were measured relative to a different hydrogenic refer-

TABLE III. Experimental intrashell intervals in Xe^{44+} and La^{47+} .

Element	Transition	Energy ^a (eV)	Energy ^b (eV)
Xenon	$(2p_{3/2}^5 3p_{1/2})_{J=2} \rightarrow (2p_{3/2}^5 3s_{1/2})_{J=1}$	89.6±0.3	89.1±0.5
	$(2p_{3/2}^5 3p_{3/2})_{J=2} \rightarrow (2p_{3/2}^5 3s_{1/2})_{J=1}$	183.2±0.3	182.9±0.5
	$(2p_{1/2}^5 3p_{3/2})_{J=2} \rightarrow (2p_{1/2}^5 3s_{1/2})_{J=1}$	184.9±0.6	186.5±1
	$(2p_{3/2}^5 3d_{5/2})_{J=1} \rightarrow (2p_{3/2}^5 3p_{3/2})_{J=2}$	159.0±0.3	157.2±0.5
	$(2p_{1/2}^5 3d_{3/2})_{J=2} \rightarrow (2p_{1/2}^5 3p_{3/2})_{J=2}$	129.0±0.7	131.3±1
Lanthanum	$(2p_{3/2}^5 3p_{1/2})_{J=2} \rightarrow (2p_{3/2}^5 3s_{1/2})_{J=1}$	96.7±0.6	
	$(2p_{1/2}^5 3p_{3/2})_{J=2} \rightarrow (2p_{1/2}^5 3s_{1/2})_{J=1}$	212.8±0.7	

^aPresent measurement.

^bDietrich *et al.*, Ref. 27.

ence line; the energy of a given $\Delta n = 0$ transition is then determined by taking the appropriate difference between two x-ray lines. The error, which we have listed in Table III, is given by the sum of the errors of the wavelengths of each x-ray line. Besides the possibility that the discrepancies of the experimental values in Table III result from the different experimental procedures, it is also possible that these discrepancies occur because the excitation mechanisms of the lines are very different in the two experiments. For example, the cross section for doubly excited states is much larger in beam-foil excitation than in low-density tokamak plasmas. Thus the contribution of unresolved satellites to the apparent neonlike lines (especially to lines 3C and 3D) may be different as well, causing different shifts in the wavelengths of the apparent resonance lines.

Finally, we have also identified one $n = 4$ to $n = 2$ transition in neonlike xenon, which is listed in Table I and is denoted by 4D. This transition is the $\Delta n = 2$ analog of transition 3D.

IV. THEORETICAL RESULTS AND COMPARISON WITH EXPERIMENT

The energy levels of neonlike silver, xenon, lanthanum, neodymium, and europium have been calculated using the multiconfigurational Dirac-Fock code developed by Grant and co-workers.^{5,6} The code offers several different choices of calculations, notably an optimal-level (OL) calculation and an extended-average-level (EAL) calculation. In the OL calculation the basis state wave functions are optimized for a particular energy level; in the EAL calculation the wave functions are obtained by minimizing the average energy of all levels weighted by their respective statistical weights. The code takes into account the interaction between any two atomic electrons due to the exchange of a transverse photon through the use of the frequency-dependent Breit operator.²⁸ Further, it explicitly calculates corrections arising from QED effects.⁶ In particular, the vacuum polarization is evaluated in second order according to a prescription given by Fullerton and Rinker.²⁹ The self-energy correction is calculated based on an effective-charge approach.⁶ This approach determines an effective nuclear charge for each orbital and interpolates among the hydrogenic self-energies tabulated by Mohr for the $1s_{1/2}$, $2s_{1/2}$, $2p_{1/2}$, and $2p_{3/2}$ levels.^{30–32} For levels with principal quantum number $n \geq 3$ the n^{-3} scaling rule³³ is used to estimate the self-energies.⁶ In order to get the self-energy correction to a given transition energy, the sum of the self-energies of every electron in both the initial and final states is calculated and then subtracted. As a result, the procedure takes into account energy shifts due to relaxation effects. Effects due to the finite nuclear size are taken into account by employing the Fermi model for the nuclear charge distribution.³⁴

The results of the MCDF calculations are listed in Table IV. All energies except those of the $3d \rightarrow 2p$ transitions labeled 3C and 3D were obtained using the EAL procedure and including all 36 singly excited states with a hole in the $n = 2$ shell and a single electron in the $n = 3$

shell. The transition energy of line 4D in xenon was calculated in similar fashion by applying the EAL procedure to the $n = 4$ spectroscopic complex. For comparison we have calculated the transition energies of lanthanum using the OL approach. The resulting energies differ from the values obtained in the EAL calculation by less than 0.2 eV. The only exceptions are transitions 3C and 3D. The theoretical energies obtained from the OL calculations are 0.7 eV lower in the case of transition 3C and 0.5 eV lower in the case of transition 3D than the values obtained from the EAL calculation. Consequently, we have recalculated the $3d \rightarrow 2p$ transition energies for all elements in the OL approach, since we deem the OL calculations to be more accurate. The resulting values are listed in Table IV. The relativistic Coulomb energies E_{Coulomb} , the Breit interaction energies E_{Breit} , and the QED corrections, which make up the total transition energy E_{total} , are listed separately in Table IV. The calculations show that the QED corrections are a significant part of E_{total} . The QED corrections are largest for the transitions involving a $2s$ -hole state, namely for the transitions labeled 3A, 3B, and E2S. In the case of lanthanum the calculated QED corrections of these levels are over 6 eV, which is about one part in 1000. The predicted size of the radiative corrections of the $3s$ levels is considerably smaller. It ranges between 0.7 eV in silver to 1.8 eV in europium for the transitions 3G and M2, and is about 30% larger for transition 3F.

In the last column of Table IV, a comparison is made between the theoretical energies and the experimental values. Here ΔE is defined as the difference between the experimental minus the theoretical energy, i.e.,

$$\Delta E \equiv E_{\text{expt}} - E_{\text{total}}.$$

The uncertainty in ΔE is listed in the table and reflects solely the uncertainty in the experimental values. For this purpose the measured wavelengths given in Table I were converted to energies using the conversion constant $hc/e = 12\,398.54 \text{ eV \AA}$.³⁵ We have included the values of ΔE for silver which we had measured earlier.³ For consistency with the data for the higher- Z elements, the experimental energies of the silver transitions were rereferenced to hydrogenic calibration lines instead of the heliumlike reference lines used in Ref. 3. The rereferencing has had the effect of increasing the value of E_{expt} by approximately 0.3 eV.

The largest deviation of the theoretical energies from the experimental values is less than 2.8 eV, or 0.5 parts per thousand. A close examination of the differences shows that the differences are not random. Instead, ΔE exhibits systematic variations which depend on the type of transition, and which to a lesser extent also depend on Z . These variations can be seen in Fig. 5, where the values of ΔE are plotted separately for different types of transitions as a function of Z . The figure shows that ΔE is generally positive for transitions into a $2p$ -vacancy state, and negative for transitions into a $2s$ -vacancy state. The values of ΔE of the $3s \rightarrow 2p$ transitions, labeled 3G and M2, are plotted in Fig. 5(a). The values vary between 1.2 and 1.8 eV. Figure 5(a) also shows the values of ΔE of the $3d, 3p \rightarrow 2s$ transitions. In this case the average

values decrease from about -1.4 eV in silver to -2.5 eV in lanthanum. The values of ΔE for the $3s \rightarrow 2p$ transitions, labeled $3F$, are shown in Fig. 5(b) and nearly equal those of $3G$ and $M2$ except for the point at $Z=60$. The values of ΔE of the $3d \rightarrow 2p$ transitions are plotted in Fig. 5(c). For transitions $3D$, ΔE equals about $+0.6$ eV, except in the case of xenon, where ΔE vanishes. For the transitions $3C$, which involve states of different angular momentum, ΔE is slightly above $+1$ eV. In Fig. 5(d) we plot ΔE for transitions of the type $3p \rightarrow 2p$. The magnitude of ΔE is found to be about 0.5 eV larger for the $2p_{J=1/2}^5$ -vacancy states than for the $2p_{J=3/2}^5$ -vacancy

states, although the values of ΔE for both types of transitions are comparable to the values found for the $3s \rightarrow 2p$ transitions. The value of ΔE for transition $4D$ is also comparable to those of the $3s \rightarrow 2p$ transitions.

The EAL scheme used to calculate the values in Table IV includes configuration interaction from the same complex only. The same holds true for the OL scheme used to calculate the energies of the transitions $3C$ and $3D$. Consequently, we do not expect the theoretical transition energies given in Table IV to agree exactly with the experimental values. Instead we expect $\Delta E \approx E_C$, where E_C is the residual electron correlation energy. In the follow-

TABLE IV. Comparison between theoretical and experimental energies. The theoretical values were obtained from an extended average level calculation, except transitions $3C$ and $3D$, which were calculated in the optimum level approach. E_{Coulomb} is the relativistic Coulomb energy, E_{Breit} is the transverse Breit correction, E_{VP} is the vacuum polarization energy, E_{SE} is the self-energy, and E_{total} is the sum of the preceding columns. ΔE is defined as the difference between the experimental energies and E_{total} . The experimental values for xenon, lanthanum, neodymium, and europium are from Table I. The experimental values of silver are from Ref. 3. The uncertainties in ΔE are indicated in parentheses and are solely due to uncertainties in the experimental values; here, $1.56(10)$ means 1.56 ± 0.10 .

Element	Key	E_{Coulomb} (eV)	E_{Breit} (eV)	E_{VP} (eV)	E_{SE} (eV)	E_{total} (eV)	ΔE (eV)
Silver	$M2$	3083.18	-4.39	-0.14	+0.83	3079.49	+1.56(10)
	$3G$	3087.72	-4.30	-0.14	+0.83	3084.12	+1.43(10)
	$E2L$	3161.95	-3.62	-0.02	-0.09	3158.23	+0.92(10)
	$E2M$	3213.26	-4.12	-0.02	-0.02	3209.11	+1.03(10)
	$3F$	3267.89	-7.29	-0.12	+1.11	3261.59	+1.25(10)
	$3D$	3339.82	-5.21	-0.02	-0.07	3334.53	+0.60(10)
	$E2U$	3392.42	-7.33	-0.00	+0.27	3385.36	+1.56(20)
	$3C$	3502.82	-7.95	-0.00	+0.19	3495.07	+1.05(10)
	$3B$	3605.64	-2.98	+0.44	-3.52	3599.59	-1.12(25)
	$3A$	3654.93	-3.73	+0.45	-3.47	3648.18	-1.64(10)
Xenon	$M2$	4214.66	-6.88	-0.26	+1.36	4208.88	+1.32(20)
	$3G$	4220.07	-6.74	-0.26	+1.36	4214.44	+1.17(20)
	$E2L$	4310.17	-5.61	-0.04	-0.23	4304.29	+0.98(20)
	$E2M$	4404.55	-6.49	-0.03	-0.11	4397.93	+0.87(30)
	$3F$	4552.50	-11.29	-0.18	+1.39	4542.42	+1.12(20)
	$3D$	4566.37	-8.79	-0.07	+0.23	4557.75	+0.05(20)
	$E2U$	4738.43	-11.91	+0.01	+0.39	4726.92	+1.50(50)
	$3C$	4868.79	-12.81	+0.02	+0.20	4856.20	+1.21(20)
	$3B$	4961.57	-4.84	+0.84	-5.98	4951.60	-2.40(40)
	$3A$	5053.18	-6.09	+0.86	-5.92	5042.03	-2.10(20)
	$E2S$	5193.35	-6.95	+0.86	-6.05	5181.22	-2.45(20)
	$4D$	5923.32	-8.50	-0.03	-0.18	5914.61	+1.66(30)
Lanthanum	$M2$	4749.90	-8.17	-0.33	+1.65	4743.04	+1.40(20)
	$3G$	4755.69	-7.99	-0.33	+1.65	4749.02	+1.34(40)
	$E2L$	4852.97	-6.63	-0.05	-0.32	4845.98	+1.08(20)
	$3D$	5146.08	-10.06	-0.04	-0.26	5135.73	+0.62(20)
	$3F$	5184.21	-14.04	-0.27	+2.17	5172.06	+1.48(20)
	$E2U$	5398.57	-14.39	+0.02	+0.43	5384.62	+1.69(40)
	$3A$	5737.04	-7.37	+1.11	-7.29	5723.49	-2.28(40)
	$E2S$	5891.32	-8.39	+1.11	-7.47	5876.58	-2.78(40)
Neodymium	$M2$	5314.44	-9.59	-0.42	+1.97	5306.39	+1.52(25)
	$3G$	5320.62	-9.38	-0.42	+1.97	5312.79	+1.38(25)
	$3D$	5766.89	-11.66	-0.04	-0.45	5754.75	+0.48(40)
	$3F$	5859.14	-16.99	-0.35	+2.67	5844.46	+2.17(40)
Europium	$M2$	5907.56	-11.15	-0.54	+2.35	5898.22	+1.69(60)
	$3G$	5914.14	-10.90	-0.54	+2.35	5905.05	+1.80(60)

ing we estimate the magnitude of E_C and compare its value to ΔE .

Ideally, the correlation contribution to the transition energy should be determined by calculating the total correlation energies of the ground state and each excited state and taking the difference. However, since such a procedure is extremely involved, the simpler approach of Chen *et al.* is used.^{2,36} Here the correlation energies of the passive electrons from the ground and excited state are assumed to cancel. The two dominant correlation corrections which remain after the cancellation are the

ground-state correlation correction E_{GS} , and, in the case of the $2s$ -hole states, the energy shift E_{CK} , due to Coster-Kronig and super-Coster-Kronig fluctuations. Hence, $E_C \approx E_{GS}$ for the $2p$ -hole states and $E_C \approx E_{GS} + E_{CK}$ for the $2s$ -hole states.

The ground-state correlation energy arises because pairs are broken in the excitation. Since all pair energies are negative and since there are more pairs in the ground state than in the excited state, this effect increases the transition energies. As a result E_{GS} is positive. Furthermore, we make use of the findings by Öksüz and Sinanoğlu^{37,38} that all external pair correlation energies are approximately constant as a function of Z and as a function of the number of electrons in a given element. This allows us to estimate the residual pair correlation energy based on a nonrelativistic calculation of the pair energies for neutral zinc performed by Jankowski *et al.*³⁹ As a result we obtain $E_{GS} = 1.7$ eV for transitions involving a $2p$ -vacancy state, and $E_{GS} = 1.0$ eV for transitions involving a $2s$ -vacancy state.

The energies of the transitions $3d, 3p \rightarrow 2s$ are affected not only by ground-state correlations but also by (super-) Coster-Kronig fluctuations of the hole state.^{2,36,40,41} This dynamic relaxation process in which the core hole fluctuates to intermediate levels of the Coster-Kronig or super-Coster-Kronig-type reduces the transition energies. The effect can be accounted for by allowing for configuration interactions with the states $(2s^2 2p^4 3l 3d)_{J=1,2}$ in the MCDF calculation and by using the OL method. The results of these calculations are given in Table V. The energy shift E_{CK} due to the (super-) Coster-Kronig-type fluctuations is obtained by subtracting E_{total} given in Table IV from E_{total} given in Table V. In the case of the $3p \rightarrow 2s$ electric dipole transitions the (super-) Coster-Kronig fluctuations reduce the transition energies by 1.9 eV. The reduction is not as large for the energies of the $3d \rightarrow 2s$ electric quadrupole transitions. In this case the reduction is 0.9 eV.

The values of the residual electron correlation energy can now be obtained by adding the values for E_{GS} and E_{CK} . As a result we obtain $E_C \approx +1.7$ eV for all transitions into a $2p$ -vacancy state, $E_C \approx -0.9$ eV in the case of the electric dipole transitions $3p \rightarrow 2s$, and $E_C \approx +0.1$ eV in the case for the electric quadrupole transitions $3d \rightarrow 2s$.

Comparing the values of E_C to those of ΔE we find that for many, but not all transitions, the agreement of the theoretical energies with the experimental data is improved. E_C and ΔE are of comparable size, in particular for the transitions $M2$, $3G$, $3F$, $4D$, and $E2U$. Thus the addition of E_C to E_{total} improves the agreement between theory and experiment in this case. The opposite is true for transitions $3D$ where the inclusion of E_C in the theoretical values worsens the agreement between theory and data. Addition of E_C to E_{total} reduces the discrepancy between theory and data for the transitions $3p \rightarrow 2s$. The remaining discrepancies for transition $3A$ range from as little as -0.74 eV in silver to -1.19 eV in xenon, and -1.36 eV in lanthanum. No improvement is achieved for the $3d \rightarrow 2s$ electric quadrupole transitions. The disagreement of the theoretical values with the data

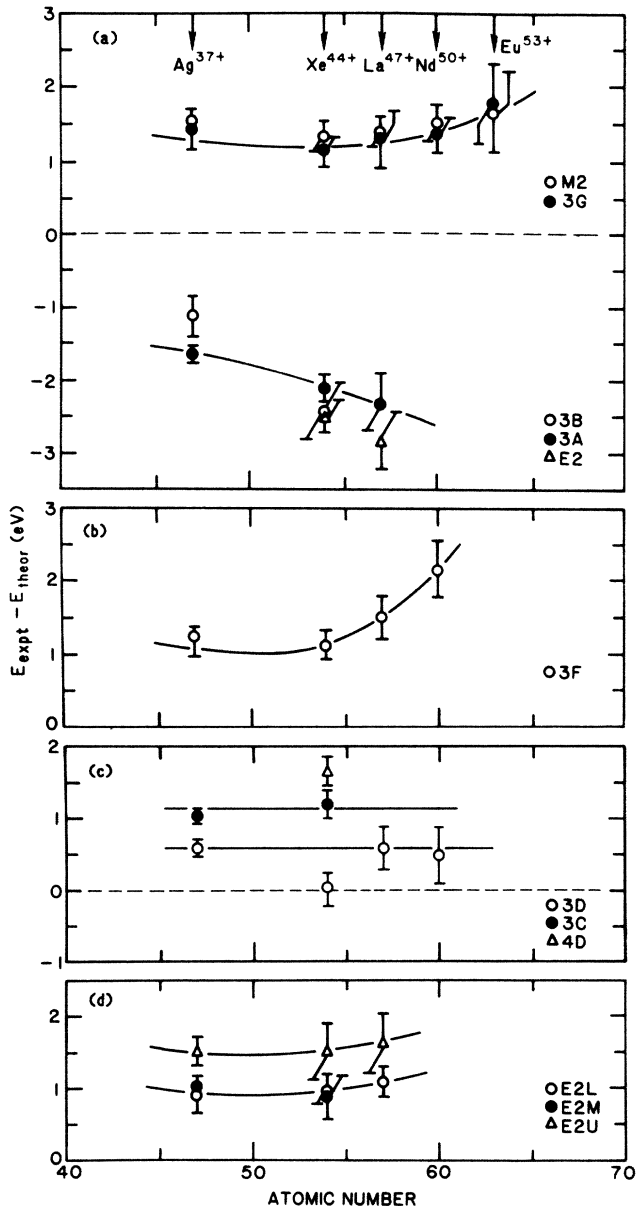


FIG. 5. Comparison of measured and theoretical energies for transitions of the type (a) $3s_{1/2} \rightarrow 2p_{3/2}$ and $3d, 3p \rightarrow 2s$; (b) $3s_{1/2} \rightarrow 2p_{1/2}$; (c) $3d, 4d \rightarrow 2p$; and (d) $3p \rightarrow 2p$. The theoretical values were calculated in the extended average level approach, except transitions $3C$ and $3D$, which were calculated in the optimum level approach. The solid lines are drawn as a visual aid only.

TABLE V. Theoretical energies of the transitions $3A$, $3B$, and $E2S$. The energies are obtained from optimal level calculations which take into account interactions with states $(2s^2 2p^4 3p 3d)_{J=1}$ in the case of transitions $3A$ and $3B$, and interactions with states $(2s^2 2p^4 3d 3d)_{J=2}$ in the case of transition $E2S$. E_{CK} is the fraction of E_{total} which arises from (super-) Coster-Kronig fluctuations.

Element	$3B$		$3A$		$E2S$	
	E_{total} (eV)	E_{CK} (eV)	E_{total} (eV)	E_{CK} (eV)	E_{total} (eV)	E_{CK} (eV)
Silver	3597.69	-1.90	3646.28	-1.90		
Xenon	4949.69	-1.91	5040.12	-1.91	5180.32	-0.90
Lanthanum			5721.57	-1.92	5875.68	-0.90

remains largest for these transitions and ranges from -2.55 eV in xenon to -2.88 eV in lanthanum.

Part of the discrepancy between the theoretical and experimental values may be due to inadequacies in treating the electron pair correlation energies. Our simple estimate is based on the nonrelativistic calculation for neutral zinc,³⁹ because no suitable relativistic calculation exists. A fully relativistic calculation of the correlation energies for high- Z neonlike systems could improve our estimate considerably.

A further cause for the discrepancy between theoretical and experimental values may be an inadequate treatment of the self-energy contribution to the transition energy. Table IV shows that the radiative corrections are largest for the $2s$ -vacancy states. Consequently, an error in the value of the self-energy will affect these levels the most, and, conversely, if there are problems with the radiative corrections, they will most likely be found in these levels. The values of the self-energy listed in Table IV are obtained from hydrogenic values which are adjusted for screening.⁶ On the other hand, the use of hydrogenic self-energies³² lowers the theoretical energies of the $3d, 3p \rightarrow 2s$ transitions by approximately 1.1, 1.7, and 2.0 eV in the case of silver, xenon, and lanthanum, respectively, and improves the agreement with the data. The improved agreement, however, may be completely fortuitous. There is no *a priori* reason to believe that the use of hydrogenic self-energies (bare or screened) is valid in a regime where the orbitals are very much nonhydrogenic, as in the case of ten-electron, neonlike systems.

V. SUMMARY

The emphasis of this paper has been to present a coherent set of wavelength data which can be used for comparison with theoretical results. In particular, we have reported on wavelength measurements of x-ray transitions in Xe^{44+} , La^{47+} , Nd^{50+} , and Eu^{53+} , which were observed in the wavelength region 2.00–2.19 and 2.29–3.00 Å. The measurements include the strong electric dipole transitions $3d \rightarrow 2p$, $3s \rightarrow 2p$, and $3p \rightarrow 2s$ as well as the weaker electric quadrupole transitions $3p \rightarrow 2p$ and $3d \rightarrow 2s$. Further, the strong magnetic quadrupole transition $(2p^5_{3/2} 3s_{1/2})_{J=2} \rightarrow \text{ground state}$ has been observed for each element. We have also identified one $\Delta n = 2$ transition of the type $4d \rightarrow 2p$ in neonlike xenon. The wavelength of each transition was determined with

high accuracy (± 0.1 mÅ for most lines) with the help of a multitude of reference spectra from hydrogenlike ions.

Together with the wavelengths of neonlike silver measured earlier,³ the data have been used for comparison with multiconfigurational relativistic atomic structure calculations. The comparisons reveal differences, the magnitudes of which depend on the particular type of transition and which vary smoothly with Z . For all transitions to $2p$ -vacancy states except transition $3D$ the magnitude ranges between $+0.9$ and $+2.2$ eV. For transition $3D$ the magnitude of the differences ranges only between 0 and $+0.6$ eV. The residual electron correlation energy for the transitions into a $2p$ -vacancy state has been estimated to equal $E_C \approx +1.7$ eV so that E_C is comparable in size to the magnitude of most differences. Consequently, adding E_C to the calculated energies improves the agreement of the theoretical values with the data for many transitions, especially in the case of the $3s \rightarrow 2p$ transitions. For the transitions into a $2s$ -vacancy state the experimental energies are significantly less than those predicted by the MCDF calculations. Inclusion of electron correlations due to ground-state correlations and (super-) Coster-Kronig-type fluctuations in the theoretical transition energies reduces the discrepancy between experimental and theoretical energies in the case of the $3p \rightarrow 2s$ transitions. The magnitude of the remaining discrepancies for transition $3A$ ranges from -0.76 eV in silver to -1.36 eV in lanthanum. Inclusion of residual electron correlations in the MCDF values does not diminish the discrepancy of the $3d \rightarrow 2s$ electric quadrupole transitions. Here the discrepancies are -2.55 and -2.88 eV in xenon and lanthanum, respectively. The discrepancies found after accounting for the additional electron correlations indicate strongly that further work is needed to resolve the differences.

The measurements presented in this paper were obtained in plasmas with electron temperatures in the range 4–6.5 keV. Based on the trends shown in Fig. 1 we can estimate that a peak electron temperature near 10 keV is needed to observe x-ray transitions in neonlike ions with atomic number $Z \approx 70$. Temperatures in this range may be achieved in tokamaks with additional electron heating power or with electron heating as a by-product of ion heating in fusion devices. High-resolution measurements of neonlike transitions in such very high-electron temperature plasmas are bound to yield new insights into our understanding of the structure of high- Z , multielectron systems.

ACKNOWLEDGMENTS

We are grateful for the support and encouragement provided by M. Eckart, H. Furth, A. Toor, and L. Wood. We have benefitted from discussions with U. Safronova from the Institute of Spectroscopy in Troitsk and with U. Feldman from the Naval Research Laboratory. We would like to thank K. Mann, J. Anastasio, H. Anderson,

and J. Gething, as well as J. Gorman, J. Lehner, and M. Saracino for their technical support. This work was supported by the Lawrence Livermore National Laboratory under Subcontract Nos. SANL-622-033 and 8-668-705, and by the U.S. Department of Energy under Contract Nos. DE-ACO2-76-CHO-3073 and W-7405-ENG-48. One of the authors (P.B.) was supported by the Fannie and John Hertz Foundation.

- ¹J. F. Seely, J. O. Ekberg, C. M. Brown, U. Feldman, W. E. Behring, J. Reader, and M. C. Richardson, *Phys. Rev. Lett.* **57**, 2924 (1986).
- ²M. H. Chen, *Phys. Rev. A* **36**, 665 (1987).
- ³P. Beiersdorfer, M. Bitter, S. von Goeler, S. Cohen, K. W. Hill, J. Timberlake, R. S. Walling, M. H. Chen, P. L. Hagelstein, and J. H. Scofield, *Phys. Rev. A* **34**, 1297 (1986).
- ⁴D. D. Dietrich, G. A. Chandler, P. O. Egan, K. P. Ziock, P. H. Mokler, S. Reusch, and D. H. H. Hoffmann, *Nucl. Instrum. Methods B* **24/25**, 301 (1987).
- ⁵I. P. Grant, B. J. McKenzie, P. H. Norrington, D. F. Mayers, and N. C. Pyper, *Comput. Phys. Commun.* **21**, 207 (1980).
- ⁶B. J. McKenzie, I. P. Grant, and P. H. Norrington, *Comput. Phys. Commun.* **21**, 233 (1980).
- ⁷K. W. Hill, S. von Goeler, M. Bitter, L. Campbell, R. D. Cowan, B. Fraenkel, A. Greenberger, R. Horton, J. Hovey, W. Roney, N. R. Sauthoff, and W. Stodiek, *Phys. Rev. A* **19**, 1770 (1979).
- ⁸J. E. Stevens, R. E. Bell, S. Bernabei, A. Cavallo, T. K. Chu, P. L. Colestock, W. Hooke, J. Hosea, F. Jobs, T. Luce, E. Mazzucato, R. Motley, R. Pinsker, S. von Goeler, and J. R. Wilson, *Nucl. Fusion* **28**, 217 (1988).
- ⁹R. E. Bell, S. Bernabei, A. Cavallo, T. K. Chu, T. Luce, R. Motley, M. Ono, J. Stevens, and S. von Goeler, *Phys. Rev. Lett.* **60**, 1294 (1988).
- ¹⁰C. Breton, C. De Michelis, M. Finkenthal, and M. Mattioli, Fontenay-aux-Roses Laboratory Report No. EUR-CEA-FC-948, 1978 (unpublished).
- ¹¹R. A. Hulse, *Nucl. Tech. Fusion* **3**, 259 (1983).
- ¹²E. S. Marmor, J. L. Cecchi, and S. A. Cohen, *Rev. Sci. Instrum.* **46**, 1149 (1975).
- ¹³J. D. Garcia and J. E. Mack, *J. Opt. Soc. Am.* **55**, 654 (1965).
- ¹⁴G. W. Erickson, *J. Phys. Chem. Ref. Data* **6**, 831 (1977).
- ¹⁵W. R. Johnson and G. Soff, *At. Data Nucl. Data Tables* **33**, 405 (1985).
- ¹⁶P. Mohr, *At. Data Nucl. Data Tables* **29**, 453 (1983).
- ¹⁷F. Bely-Dubau, A. H. Gabriel, and S. Volonté, *Mon. Not. R. Astron. Soc.* **189**, 801 (1979).
- ¹⁸M. Bitter, S. von Goeler, S. Cohen, K. W. Hill, S. Sesnic, F. Tenney, J. Timberlake, U. I. Safronova, L. A. Vainshtein, J. Dubau, M. Loulergue, F. Bely-Dubau, and L. Steenman-Clark, *Phys. Rev. A* **29**, 661 (1984).
- ¹⁹M. Bitter, K. W. Hill, M. Zarnstorff, S. von Goeler, R. Hulse, L. C. Johnson, N. R. Sauthoff, S. Sesnic, and K. M. Young, *Phys. Rev. A* **32**, 3011 (1985).
- ²⁰L. A. Vainshtein and U. I. Safronova, *Phys. Scr.* **31**, 519 (1985).
- ²¹Y. Conturie, B. Yaakobi, U. Feldman, G. A. Doschek, R. D. Cowan, *J. Opt. Soc. Am.* **71**, 1309 (1981).
- ²²E. V. Aglitskii, P. S. Antsiferov, A. M. Panin, and S. A. Ulitin, *Opt. Spektrosk.* **60**, 197 (1986) [*Opt. Spectrosc. (USSR)* **60**, 122 (1986)].
- ²³J.-C. Gauthier, J. Geindre, P. Monier, E. Luc-koenig, and J. Wyart, *J. Phys. B* **19**, L385 (1986).
- ²⁴D. L. Matthews, P. L. Hagelstein, M. D. Rosen, M. J. Eckart, N. M. Ceglio, A. U. Hazi, H. Medeck, B. J. MacGowan, J. E. Trebes, B. L. Whitten, E. M. Campbell, C. W. Hatcher, A. M. Hawryluk, R. L. Kauffman, L. D. Pleasance, G. Rambach, J. H. Scofield, G. Stone, and T. A. Weaver, *Phys. Rev. Lett.* **54**, 110 (1985).
- ²⁵M. D. Rosen, P. L. Hagelstein, D. L. Matthews, E. M. Campbell, A. U. Hazi, B. L. Whitten, B. MacGowan, R. E. Turner, R. W. Lee, G. Charatis, G. E. Busch, C. L. Shepard, and P. D. Rockett, *Phys. Rev. Lett.* **54**, 106 (1985).
- ²⁶T. N. Lee, E. A. McLean, and R. C. Elton, *Phys. Rev. Lett.* **59**, 1185 (1987).
- ²⁷D. D. Dietrich, G. A. Chandler, R. J. Fortner, C. J. Hailey, and R. E. Stewart, *Phys. Rev. Lett.* **54**, 1008 (1985).
- ²⁸I. P. Grant and B. J. McKenzie, *J. Phys. B* **13**, 2671 (1980).
- ²⁹L. W. Fullerton and G. A. Rinker, Jr., *Phys. Rev. A* **13**, 1283 (1976).
- ³⁰P. J. Mohr, *Ann. Phys. (N.Y.)* **88**, 52 (1974).
- ³¹P. J. Mohr, *Phys. Rev. Lett.* **34**, 1050 (1975).
- ³²P. J. Mohr, *Phys. Rev. A* **26**, 2338 (1982).
- ³³H. A. Bethe, *Phys. Rev.* **72**, 339 (1947).
- ³⁴M. H. Chen, B. Crasemann, M. Aoyagi, K.-N. Huang, and H. Mark, *At. Data Nucl. Data Tables* **26**, 561 (1981).
- ³⁵Value based on a 1984 revision of the Physical Constants by B. N. Taylor, in *X-Ray Data Booklet*, edited by D. Vaughan (Center for X-Ray Optics, Lawrence Berkeley Laboratory, University of California, Berkeley, 1986); E. R. Cohen and B. N. Taylor, *J. Chem. Ref. Data* **2**, 663 (1973).
- ³⁶M. H. Chen, B. Crasemann, N. Mårtensson, and B. Johansson, *Phys. Rev. A* **31**, 556 (1985).
- ³⁷İ. Öksüz and O. Sinanoğlu, *Phys. Rev.* **181**, 42 (1969).
- ³⁸İ. Öksüz and O. Sinanoğlu, *Phys. Rev.* **181**, 54 (1969).
- ³⁹K. Jankowski, P. Malinowski, and M. Polasik, *J. Chem. Phys.* **76**, 448 (1982).
- ⁴⁰M. Ohno and G. Wendin, *J. Phys. B* **11**, 1557 (1978).
- ⁴¹M. Ohno and G. Wendin, *J. Phys. B* **12**, 1305 (1979).